Cell Reports
Report



# Germ Plasm Anchoring Is a Dynamic State that Requires Persistent Trafficking

Kristina S. Sinsimer,[1,3] Jack J. Lee,[1,3] Stephan Y. Thiberge,[2] and Elizabeth R. Gavis[1,*]
[1]Department of Molecular Biology, Princeton University, Princeton, NJ 08544, USA
[2]Lewis-Sigler Institute for Integrative Genomics, Princeton University, Princeton, NJ 08544, USA
[3]These authors contributed equally to this work
*Correspondence: gavis@princeton.edu
http://dx.doi.org/10.1016/j.celrep.2013.10.045


## SUMMARY

**Localized cytoplasmic determinants packaged as ribonucleoprotein (RNP) particles direct embryonic patterning and cell fate specification in a wide range of organisms. Once established, the asymmetric distributions of such RNP particles must be maintained, often over considerable developmental time. A striking example is the *Drosophila* germ plasm, which contains RNP particles whose localization to the posterior of the egg during oogenesis results in their asymmetric inheritance and segregation of germline from somatic fates in the embryo. Although actin-based anchoring mechanisms have been implicated, high-resolution live imaging revealed persistent trafficking of germ plasm RNP particles at the posterior cortex of the *Drosophila* oocyte. This motility relies on cortical microtubules, is mediated by kinesin and dynein motors, and requires coordination between the microtubule and actin cytoskeletons. Finally, we show that RNP particle motility is required for long-term germ plasm retention. We propose that anchoring is a dynamic state that renders asymmetries robust to developmental time and environmental perturbations.**

## INTRODUCTION

Localized cytoplasmic determinants, often in the form of mRNA, play important roles in generating asymmetries of gene expression necessary for developmental events including embryonic patterning, asymmetric cell division, and cell fate determination. For example, both abdominal and germ cell development during *Drosophila* embryogenesis are directed by determinants contained within germ plasm ribonucleoprotein (RNP) particles that are localized at the posterior pole of the embryo. In animals like *Drosophila* and *Xenopus*, localized germ plasm assembly occurs during oogenesis, long before germ plasm function is needed in the embryo (Becalska and Gavis, 2009; King et al., 2005). Although much attention has been focused on the intracellular trafficking mechanisms that generate such localized asymmetric distributions, how they are subsequently maintained is poorly understood.

Assembly of the *Drosophila* germ plasm occurs in two phases, beginning during midoogenesis with the kinesin-dependent transport of *oskar* (*osk*) mRNA to the posterior of the oocyte and its translation there. Osk protein then recruits other germ plasm proteins such as the RNA-helicase Vasa (Vas) (Mahowald, 2001; Becalska and Gavis, 2009). During this initial phase of localization, the oocyte is supported by nurse cells that supply it with maternal RNAs and proteins including those required for the germ plasm. The transition between midoogenesis and the late, vitellogenic stages of oogenesis is defined by physiological changes including apoptosis of the nurse cells and the deposition of their contents into the oocyte. This nurse cell "dumping" is accompanied by reorganization of the microtubule cytoskeleton into cortical bundles that mediate ooplasmic streaming, a churning of the oocyte cytoplasm that mixes the nurse cell and oocyte contents (Theurkauf et al., 1992). During this period of oogenesis, additional germ plasm RNAs, such as the abdominal determinant *nanos* (*nos*), become localized to the site nucleated by Osk. Because the cytoarchitecture of the oocyte no longer supports long-range directed transport, localization of these mRNAs is achieved by a mechanism involving diffusion and entrapment of RNP particles by association with germ plasm proteins like Vas (Forrest and Gavis, 2003; Sinsimer et al., 2011). Moreover, continued accumulation of *osk* mRNA and Vas protein at the posterior together with *nos* and other germ plasm mRNAs during this late phase results in amplification of the germ plasm that is essential for robust germ cell formation and abdominal segmentation during embryogenesis (Sinsimer et al., 2011).

Previous studies have identified roles for the actin cytoskeleton in the physical anchoring of localized mRNAs in a variety of contexts (López de Heredia and Jansen, 2004; Martin and Ephrussi, 2009). In *Drosophila*, actin has been implicated in the anchoring of *osk* mRNA during midoogenesis, in the retention of posteriorly localized germ plasm during ooplasmic streaming, and in maintaining the association of germ plasm with the posterior pole during embryogenesis (Babu et al., 2004; Forrest and Gavis, 2003; Jankovics et al., 2002; Lantz et al., 1999; Vanzo

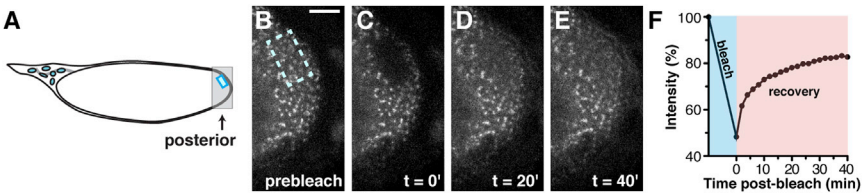


**Figure 1. A Dynamic State of Localized Germ Plasm**

(A) Cartoon represents a stage 13 oocyte. Nurse cell dumping and ooplasmic streaming are completed, and only nurse cell remnants remain at the anterior. The gray box delineates the region of the oocyte imaged in the FRAP experiment, with the photobleached 3D ROI indicated by the blue rectangle.

(B–E) FRAP experiment was performed on *osk*GFP* at the posterior of a stage 13 oocyte. Confocal z series were collected prior to photobleaching of the 3D ROI (prebleach), immediately after photobleaching (t = 0′), or during the recovery period as indicated. Posterior is to the right. Scale bar, 10 μm.

(F) Quantification of the FRAP experiment in (B)–(E) is shown. The photobleach period is indicated by blue shading, the recovery period by pink shading. Similar results were observed for *osk*GFP* in two additional oocytes as well as for oocytes expressing *nos*GFP*.

et al., 2007). Alternatively, dynein functions as a static anchor for several mRNAs in *Drosophila* oocytes and embryos (Delanoue and Davis, 2005; Delanoue et al., 2007). Although these and other studies have led to the prevailing idea that localized RNP particles become affixed or tethered to stable cytoskeletal elements, the exact mechanisms are not clear. Hence, in high-resolution imaging experiments to investigate the late phase of *Drosophila* germ plasm RNP particle assembly, we were surprised to observe dynamic behavior of RNP particles at the posterior oocyte cortex. Quantitative analysis of germ plasm RNP particle motility revealed roles for both kinesin and dynein motors as well as an interplay between the actin and microtubule cytoskeletons. Moreover, we show that motility makes retention of the germ plasm robust to developmental time and environmental perturbation.

## RESULTS AND DISCUSSION

### Localized Germ Plasm Is Motile

In the course of investigating the late phase of germ plasm mRNA localization, we used fluorescence recovery after photobleaching (FRAP) to monitor *osk* and *nos* mRNAs in late-stage oocytes following the completion of nurse cell dumping and ooplasmic streaming. Fluorescence from localized *osk* or *nos* mRNA labeled in vivo with GFP via the MS2/MCP system (*osk*GFP*, *nos*GFP*) (Forrest and Gavis, 2003) was irreversibly inactivated in a small three-dimensional (3D) region of interest (ROI) at the oocyte posterior, and fluorescence recovery in the ROI was monitored over time. Although ooplasmic streaming had visibly ceased and germ plasm accumulation appeared to be complete, fluorescence in the ROI increased over time, suggesting an ongoing local redistribution of germ plasm RNP particles (Figure 1; data not shown). These results were surprising because previous studies suggested that various germ plasm components become affixed to the cortical actin cytoskeleton (Babu et al., 2004; Forrest and Gavis, 2003; Jankovics et al., 2002; Polesello et al., 2002; Vanzo et al., 2007).

To determine the basis for the observed recovery, we analyzed the behavior of germ plasm RNP particles at high temporal and spatial resolution by using time-lapse two-photon microscopy of fluorescently labeled RNA or protein components. Individual *nos*GFP*, *osk*GFP*, and GFP-Vas particles could be detected deep within late-stage oocytes (approximately 50 μm from the cortical surface). In addition to particles that appeared static or jiggling in place, we reproducibly observed motile particles with long, directed trajectories suggestive of active transport (Figure 2A; Movie S1). Measurement of net displacement by manual tracking of individual particles showed long-range movements beyond what would be expected by diffusion (Fusco et al., 2003) (Figure 2B). Moreover, the average velocities of particles during periods of sustained movement are consistent with active transport, with *nos* and Vas particles traveling at velocities up to 0.9 and 0.8 μm/s, respectively, and the *osk* particles reaching 0.4 μm/s.

For subsequent studies to investigate the mechanism of germ plasm RNP transport, we sought motility parameters that would best allow us to compare the effects of pharmacological and genetic perturbations. In addition, we adapted a semiautomated single-particle tracking algorithm (Jaqaman et al., 2008) that allowed us to reliably quantify the behavior of all particles within defined regions of the posterior cortex. Particles detected using GFP-Vas exhibited the greatest signal-to-noise ratio and were therefore most amenable to analysis. Quantification of GFP-Vas particles undergoing sustained runs showed that velocity was often nonuniform over the duration of a run due to pausing of particles. Moreover, in addition to particles with linear trajectories, a substantial number followed multidirectional or curved trajectories. Consequently, as measures for the "motility" of an individual particle, we extracted both the maximum instantaneous velocity (velocity) and the maximum displacement of a particle from its starting point (displacement) and plotted their distributions (see Experimental Procedures). GFP-Vas particles exhibited instantaneous velocities of up to 0.87 μm/s and maximum displacements up to 6.5 μm (Figure 2C; Table S1). Mean-squared displacements calculated for a subset of sustained runs were best fit by quadratic models, in agreement with directed transport (Figure S1A).

### Germ Plasm Motility Is Dependent on a Population of Cortical Microtubules

Osk protein induces formation of F-actin projections at the posterior cortex of the oocyte that have been proposed to anchor germ plasm components (Vanzo et al., 2007). To determine whether these F-actin structures could instead mediate germ plasm RNP particle motility, we disrupted the actin cytoskeleton in late-stage oocytes by acute treatment with latrunculin A (latA). The efficacy of latA treatment was confirmed in live oocytes using the F-actin-binding protein GFP-Moesin and the actin motor MyoV-GFP (see below; Figure 4A; data not shown). Actin depolymerization did not significantly alter the

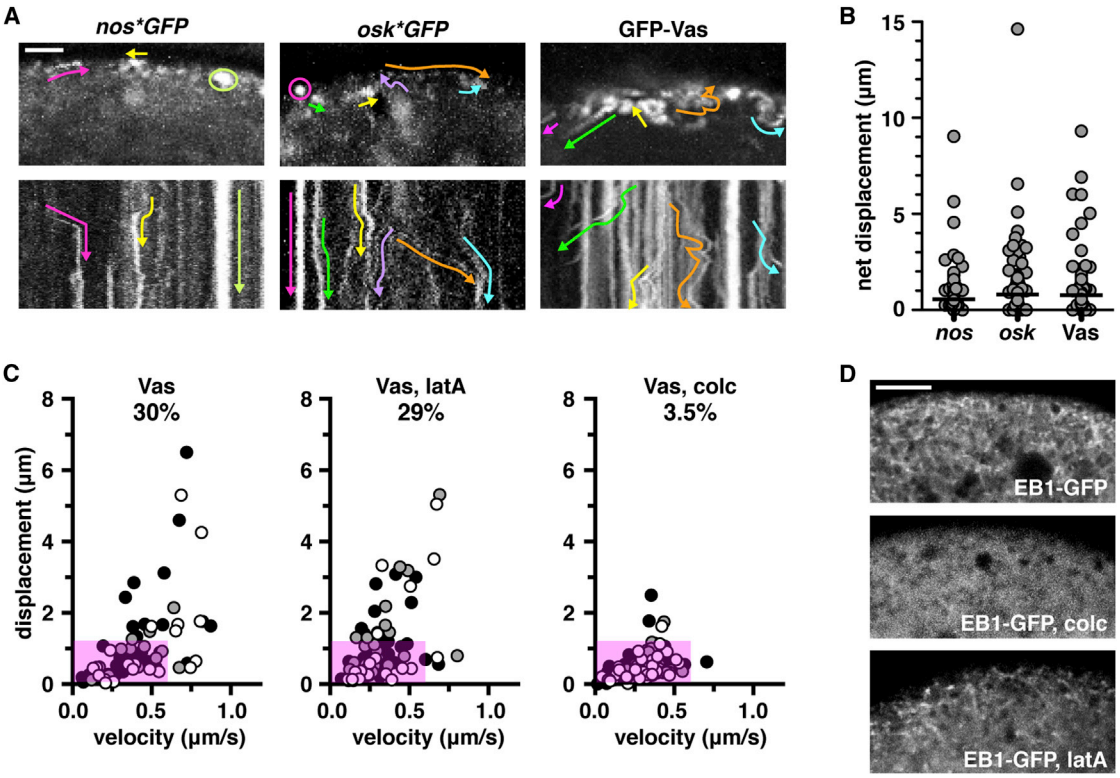


**Figure 2. Active Transport of Germ Plasm RNP Particles on Cortical Microtubules**

(A) Time-lapse two-photon imaging of *nos*GFP*, *osk*GFP*, and GFP-Vas in late-stage oocytes. Representative stage 12–13 oocytes are shown. Top row shows trail images generated by the superposition of consecutive frames spanning 20, 73, and 100 s for *nos*GFP*, *osk*GFP*, and GFP-Vas, respectively. A moving particle appears as a sequence of dots (fast movements) or a solid line (slower movements). Arrows indicate motile particles, whereas circles outline static particles; oocytes are oriented posterior end up. Bottom row presents corresponding kymographs showing movement in x direction (horizontal axis) over time (vertical axis), with later time points toward the bottom. Colored arrows mark trajectories of particles labeled with the same color in the trail images; vertical line segments result from static behavior, whereas angled segments correspond to movement in the x axis. Scale bar, 5 μm.

(B) Net displacement of *nos*GFP*, *osk*GFP*, and GFP-Vas particles is shown. Initial and final positions of all particles observed over a 100 s time period were identified and used to calculate net displacements. For each germ plasm component, data for all particles observed in three oocytes are plotted, with each circle representing the value for one particle. Horizontal lines indicate median net displacement. Long-range particle movements were observed for all three germ plasm components.

(C) Quantitative analysis of GFP-Vas motility is shown. The maximum displacement from an initial position (y axis) and the maximum instantaneous velocity (x axis) were determined for all identified particles in a 100 s time series. For each condition, data from three oocytes are plotted. Each circle represents one particle, shaded to identify the oocyte from which it originated. The magenta box denotes the "immotile" population as described in the text. The percentage of motile particles, noted below each title, was significantly reduced in colcemid (colc)-treated oocytes as compared to untreated samples ($p = 1.0 \times 10^{-31}$) but remained similar following latA treatment. Statistical analysis was performed using Pearson's chi-square test. The y axis label for all plots is located at the left. Distributions are also shown as heatmaps in Figure S1. Additional statistical analysis is provided in Table S1.

(D) Time-lapse confocal imaging of EB1-GFP. Trail images generated by superposition of consecutive frames spanning 10 s show dynamic EB1-GFP-labeled microtubules as short linear segments. EB1-GFP tracks persist after latA treatment but are eliminated by colcemid treatment. In all panels, the oocyte is oriented posterior end up. Scale bar, 5 μm.

See also Movies S1, S2, and S3, Figure S1, and Table S1.

distribution of GFP-Vas particle displacements or the frequency of long-range movements (Figures 2C and S1B; Movie S2), although median velocity was slightly reduced (Table S1). Thus, it is unlikely that actin filaments provide tracks for germ plasm RNP particle transport.

Microtubules mediate a variety of directed mRNA transport events during midoogenesis, including the initial posterior localization of *osk* (Becalska and Gavis, 2009). However, there is no prior evidence for microtubules at the posterior of late-stage oocytes that could provide the tracks on which germ plasm RNP particles travel. Through live confocal imaging of the plus-end-binding protein EB1-GFP, we observed a population of short, dynamic microtubules along the entire cortex of late-stage oocytes that could mediate trafficking of RNP particles upon their accumulation at the posterior (Figure 2D; Movie S3).

For determining whether these microtubules are indeed important for germ plasm RNP particle motility, late-stage oocytes were treated acutely with the microtubule-depolymerizing drug colcemid. Colcemid treatment resulted in the loss of EB1-GFP tracks (Figure 2D; Movie S3) and significant reductions in both median GFP-Vas particle velocity and displacement compared to mock-treated control oocytes (Table

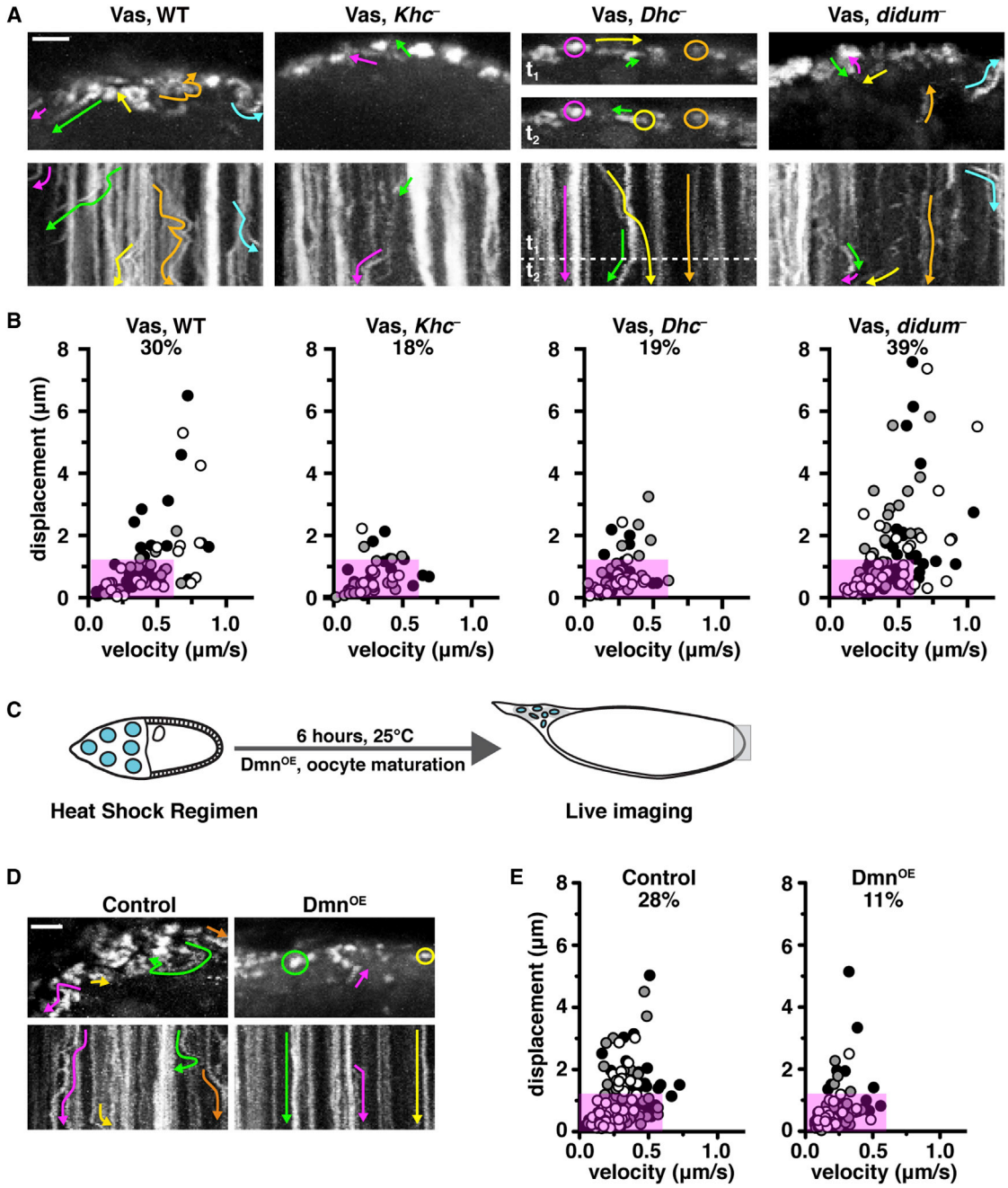


**Figure 3. Analysis of Motor Protein Requirements for Germ Plasm Motility**

(A and B) Time-lapse two-photon imaging shows GFP-Vas particles in stage 12–13 wild-type (WT), *Khc*, *Dhc*, or *didum* mutant oocytes.

(A) Top row shows trail images spanning 100 s. Display of the short, overlapping movements in *Dhc* mutants is clarified by presenting trail images and corresponding kymographs in two time segments ($t_1$ and $t_2$). Arrows indicate dynamic movements, whereas circles outline static particles; oocytes are oriented posterior end up. Bottom row presents corresponding kymographs showing changes in x position (horizontal axis) over time (vertical axis). Arrows indicating distinct particle trajectories are shown as described in the legend for Figure 2. Scale bar, 5 µm.

(B) Quantitative analysis of GFP-Vas motility is shown. The maximum displacement and the maximum instantaneous velocity were determined for all identified particles in a 100 s time series. Data from three oocytes for each genotype are plotted as in Figure 2C. The percentage of motile particles, indicated for each genotype, was significantly reduced in *Khc* and *Dhc* mutant oocytes, as compared to wild-type, whereas it increased in *didum* mutant oocytes ($p = 1.3 \times 10^{-2}$, $6.2 \times 10^{-3}$, and $3.2 \times 10^{-10}$, respectively). Statistical analysis was performed using Pearson's chi-square test. Additional details are provided in Table S1.

(C) Regimen for acute disruption of dynein by Dmn overexpression is presented. *Dmn* expression was induced at stage 10, prior to nurse cell dumping, by heat shocking adult females (see Experimental Procedures). Affected oocytes were subject to a 6 hr maturation period to allow production and localization of Dmn protein in late-stage oocytes. The gray box indicates the area visualized by two-photon imaging.

*(legend continued on next page)*

S1; Movie S2). Based on the behavior of GFP-Vas particles in colcemid-treated oocytes, we defined an "immotile" population encompassing static and jiggling particles (Figure 2C, magenta box). Applying this definition across experimental conditions, we found that 30% of particles in mock-treated late-stage oocytes were motile. This motile fraction was reduced 8.6-fold following microtubule disruption (3.5% motile) but was unaffected by actin depolymerization (29% motile) (Figures 2C and S1B; Table S1).

Taken together, these results indicate that microtubules are the primary cytoarchitecture on which germ plasm RNPs undergo long-range movements. Moreover, the requisite microtubules are indeed present at the oocyte cortex. We note that although the motile fraction is unaffected, the density of EB1 tracks appears to be decreased by latA treatment (Figure 2D; Movie S3), suggesting that these microtubules are in excess and that the cortical actin cytoskeleton may play a role in their organization or anchoring.

### Germ Plasm Motility Requires Dynein and Kinesin

To determine whether motors mediate microtubule-dependent germ plasm RNP particle motility in late-stage oocytes, we took advantage of mutations that disrupt motor protein activity. The initial localization of *osk* mRNA during midoogenesis is mediated by the plus-end motor kinesin, and a null mutation in *Kinesin heavy chain* (*Khc*), the force-generating component of kinesin, causes mis-localization of germ plasm around the entire oocyte cortex during midoogenesis (Cha et al., 2002). Visualization of GFP-Vas in *Khc* mutant germline clones showed that this aberrant pattern persisted in late-stage oocytes (data not shown). Despite the paucity of GFP-Vas particles at any one cortical location, we observed examples of dynamic behavior, and these occurred regardless of where on the cortex the particles were located (Movie S4). Quantification of the small population of GFP-Vas particles at the posterior cortex of *Khc* mutant oocytes showed a 1.7-fold reduction in the motile fraction as compared to wild-type oocytes (18% motile; Figures 3A, 3B, and S1B; Table S1) and a 36% reduction in the median velocity of the motile particles (Table S1).

The finding that germ plasm RNP particle motility is reduced but not abolished in the complete absence of kinesin function suggested the involvement of a second motor. We therefore tested whether the minus-end motor dynein might be required. Unlike kinesin, dynein is essential during early oogenesis, and complete abrogation of dynein activity precludes egg development (McGrail and Hays, 1997). Consequently, we first examined the effect of hypomorphic mutations in *Dynein heavy chain* (*Dhc*); these eggs have reduced dynein activity but still complete oogenesis (Gepner et al., 1996). Quantification of GFP-Vas in late-stage *Dhc* mutant oocytes showed a 1.6-fold decrease in the motile fraction (19%) as compared to wild-type (Figures 3A, 3B, and S1B; Table S1; Movie S4). Moreover, the median velocity of motile particles in *Dhc* mutants was half that of wild-type oocytes (Table S1). In a second approach, we disrupted dynein activity acutely in late-stage oocytes by heat shock-inducible expression of p50/Dynamitin (Dmn), a component of the dynactin complex that interferes with dynein activity when overexpressed (Figure 3C) (Duncan and Warrior, 2002). Although heat shock alone had a minor effect on GFP-Vas particle motility, there was a 2.4-fold decrease in the motile fraction when dynein was inactivated as compared to heat-shocked wild-type controls (28% versus 11%) (Figures 3D, 3E, and S1B; Table S1; Movie S5). Moreover, the median velocity of the motile population in late oocytes overexpressing Dmn was reduced by 30% compared to control oocytes (Table S1). Thus, we conclude that both kinesin and dynein contribute to germ plasm RNP motility. The comparable loss of motility in null kinesin and hypomorphic dynein mutants, however, suggests that dynein-mediated transport predominates.

Both of these motors are also involved in transport events during midoogenesis: dynein for movement of mRNAs from nurse cells to oocyte and anteriorly directed transport within the oocyte, kinesin for posterior transport of *osk* (Becalska and Gavis, 2009). Our previous work indicated that the bulk of germ plasm mRNA localization occurs not by motor-dependent transport, however, but by diffusion and entrapment of transcripts that enter the oocyte during nurse cell dumping (Forrest and Gavis, 2003; Sinsimer et al., 2011). We have not been able to resolve particles containing kinesin or dynein in late oocytes using current GFP fusions. Thus, the important question of when and where the association of motors with germ plasm RNP particles occurs awaits the development of new methods for visualization of motors in *Drosophila* oocytes.

The association of localized germ plasm RNP complexes with dynein in late-stage oocytes may serve a second purpose, providing preassembled transport particles for germ cell inheritance in the early embryo. The process of germ cell formation initiates when centrosomes and/or astral microtubules associated with nuclei that migrate to the posterior of the syncytial embryo induce release of germ plasm from the posterior cortex. Recruitment of germ plasm to the centrosomes by dynein-dependent transport on astral microtubules is required for these nuclei to induce germ cell formation and for the inheritance of the germ plasm by the newly formed germ cells (Lerit and Gavis, 2011). The prior coupling of germ plasm RNP particles to dynein in

(D) Time-lapse two-photon imaging of GFP-Vas particles in late-stage oocytes dissected from wild-type females (Control) or females overexpressing Dmn ($Dmn^{OE}$) subjected to the regimen shown in (C). Top row shows trail images spanning 100 s. Arrows indicate motile particles, whereas circles outline static particles; oocytes are oriented posterior end up. Bottom row shows kymographs corresponding to particles in trail images (x position on horizontal axis, time on vertical axis). Scale bar, 5 μm.

(E) Quantitative analysis of GFP-Vas motility is shown. The maximum displacement and the maximum instantaneous velocity were determined for all identified particles in a 100 s time series. For each genotype, data from three oocytes are plotted as in Figure 2C. The percentage of motile particles is significantly reduced in $Dmn^{OE}$ oocytes as compared to control oocytes ($p = 1.9 \times 10^{-12}$). Statistical analysis was performed using Pearson's chi-square test. Additional details are provided in Table S1. The y axis label for all plots is located at the left.

See also Movies S4 and S5, Figure S1, and Table S1.

the oocyte may allow their rapid accumulation on astral microtubules upon release from the cortex.

## Myosin V Restricts Germ Plasm Motility

The class V unconventional myosin, myosin V (MyoV), counteracts kinesin function to promote *osk* localization during midoogenesis and has been proposed to mediate entrapment of *osk* at the posterior cortex; in neither case is the mechanism known (Krauss et al., 2009). Although actin is not required for local germ plasm RNP particle transport, it is required during midoogenesis to maintain the germ plasm at the posterior cortex against the forces of ooplasmic streaming (Forrest and Gavis, 2003). We therefore investigated whether MyoV might contribute to germ plasm localization by regulating germ plasm RNP motility.

Live two-photon imaging of MyoV-GFP in late-stage oocytes revealed jiggling MyoV-GFP particles at the posterior cortex as well as MyoV-GFP undergoing long-range movements further away from the cortex (Figure 4A; Movie S6). The average velocities of these motile particles never exceeded 0.21 μm/s, far slower than speeds observed for the fastest-moving germ plasm RNP particles. In contrast to GFP-Vas particles, MyoV-GFP particles continued to exhibit long-range linear trajectories following microtubule disruption. Motility was, however, largely eliminated by actin depolymerization (Figure 4A; Movie S6). These data suggest that MyoV does not itself transport germ plasm RNP particles nor is it transported together with the particles.

In oocytes with a null mutation in *didum*, which encodes MyoV, the fraction of motile GFP-Vas particles was increased 1.3-fold compared to wild-type (39% motile; Figures 3A, 3B, and S1B; Table S1; Movie S4). Moreover, the maximum velocity (1.07 μm/s) and displacement (7.6 μm) exceeded what was observed in wild-type oocytes (Table S1). Together, these results suggest that germ plasm RNP particles moving on microtubules are restrained through an interaction with MyoV and the actin cytoskeleton. Moreover, MyoV may restrict the initiation of movement because reduction of MyoV activity led to an increase in the motile fraction.

MyoV mediates long-range actin-based transport of mRNAs in yeast and facilitates transport of dendritic RNP particles to actin-rich spines (Hammer and Sellers, 2012). In contrast, our results favor a tethering function for MyoV in germ plasm RNP particle localization, more similar to its proposed role as a dynamic tether for the reversible attachment of vesicles to F-actin along the cell cortex following delivery on microtubules (Woolner and Bement, 2009).

## Dynein-Mediated Local Trafficking Is Important for Germ Plasm Anchoring

Under conditions of stress such as nutrient deprivation or in the absence of potential mates, female flies will hold mature eggs until conditions improve to increase the likelihood of survival for their progeny. Notably, females can hold mature eggs for at least 15 days without consequence to the viability or fertility of their progeny (Wyman, 1979). Thus, sustaining germ plasm localization through such a delay of fertilization and the onset of embryogenesis is biologically crucial. We hypothesized that the persistent trafficking of germ plasm might provide a mechanism for retaining germ plasm at the posterior over long periods of time.

Because dynein is a major mediator of germ plasm RNP motility and can be manipulated acutely, we tested whether compromising dynein function in held eggs by inducible Dmn overexpression would lead to a progressive loss of germ plasm from the posterior using the experimental design outlined in Figure 4B (see also Experimental Procedures). We took advantage of a single-molecule fluorescent in situ hybridization (smFISH) method to detect endogenous *nos* and *osk* mRNAs in mature oocytes (Little et al., 2011; Raj et al., 2008). smFISH provides a major advance for mRNA analyses during the vitellogenic stages of *Drosophila* oocytes, which are largely impervious to standard molecular probes. The amount of localized germ plasm was quantified by measuring fluorescence intensity for each probe.

More than 70% of mature oocytes from wild-type control or Dmn-overexpressing females, dissected immediately following heat shock, exhibited robust germ plasm accumulation (Figures 4C and 4D, t = 0 hr; data not shown). We did observe a spreading of *nos* and *osk* along the cortex in some oocytes overexpressing Dmn, likely due to an immediate effect of dynein inhibition on germ plasm retention following the 2 hr heat shock regimen (see Figure 4C and Experimental Procedures). Examination of wild-type control oocytes held for 18 hr showed little effect of the holding period alone on localization of the germ plasm RNAs (Figures 4C and 4D, t = 18 hr; data not shown). In contrast, inhibition of dynein function in held oocytes led to a dramatic loss of both *nos* and *osk* from the posterior cortex, with robust localization persisting in fewer than 30% (Figures 4C and 4D, $Dmn^{OE}$). Thus, we conclude that dynein-mediated motility is required for long-term retention of germ plasm at the posterior cortex of the oocyte.

Similarly, we tested the effect of MyoV loss on germ plasm components in held oocytes. In mature *didum* mutant oocytes, *nos* mRNA was properly localized to the posterior, and unlike the case for Dmn overexpression, *nos* persisted during the holding period (Figures 4E and 4F). Together, these data support a model in which enhanced dynein-mediated motility facilitates *nos* RNP particle accumulation at the posterior. In contrast, *osk* mRNA was no longer confined to the posterior cortex in *didum* mutant oocytes but often had a graded or diffuse distribution (Figures 4E, 4F, and S2). Thus, a requirement for MyoV function in entrapment and/or retention of *osk* extends into late oogenesis. Strikingly, a tight cortical distribution of *osk* was largely restored in *didum* mutant oocytes held for 18 hr (Figures 4E and 4F). This suggests that given sufficient time, microtubule-based motility of *osk* RNP particles allows localization to recover in the absence of MyoV.

## Conclusions

In the most common mRNA localization paradigm, transcripts are transported in RNP particles to a particular subcellular localization, where they become affixed or anchored to cytoskeletal components (Martin and Ephrussi, 2009; Medioni et al., 2012). The cortical actin cytoskeleton has been implicated in static anchoring of mRNAs in a variety of cell types, including oocytes, fibroblasts, and budding yeast. In the *Drosophila* oocyte, actin is required for anchoring of *osk* mRNA during midoogenesis and again for retention of germ plasm RNP components at the posterior cortex against the forces of ooplasmic streaming. Here,

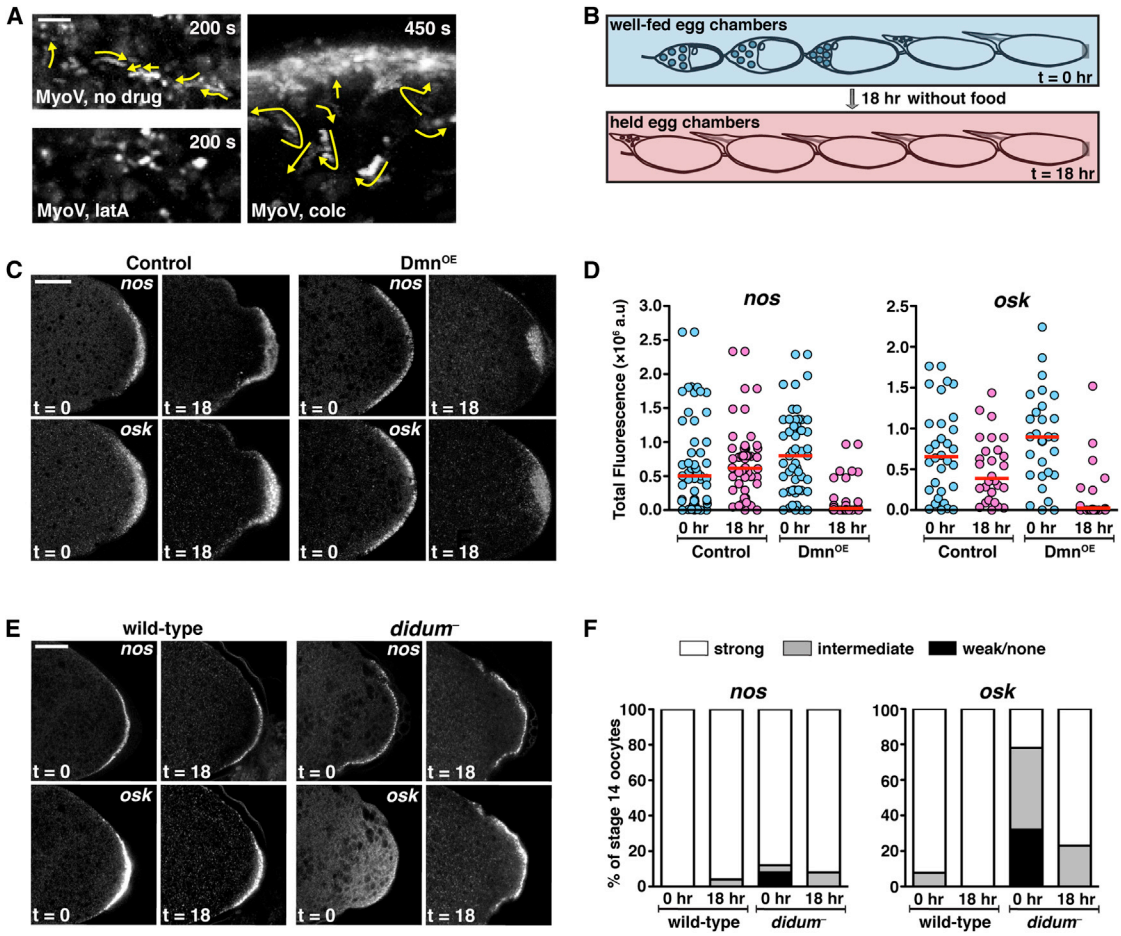


**Figure 4. Dynein-Mediated Motility Is Essential for Germ Plasm Retention**

(A) Trail images from time-lapse two-photon imaging of MyoV-GFP (superposition of consecutive frames spanning the indicated time periods) are shown. Arrows indicate long-range movements. MyoV-GFP tracks detected in the vicinity of the cortex (five out of five oocytes) were eliminated by latA (three out of three oocytes), but not by colcemid (seven out of nine oocytes). Oocytes are oriented posterior end up. Scale bar, 5 μm.

(B) Regimen for Dmn overexpression with nutrient deprivation is presented. Blue box: ovaries dissected from females at t = 0 hr, just after completion of the heat shock regimen (see Experimental Procedures), contain egg chambers spanning all stages of oogenesis. Pink box: ovaries dissected from nutrient-deprived females at t = 18 hr are enriched for late-stage egg chambers. The posterior region of late-stage oocytes imaged at each time point is delineated by the gray boxes.

(C) Confocal images show the posterior regions of oocytes from wild-type females (Control) or females overexpressing Dmn ($Dmn^{OE}$). Females were heat shocked as described in Experimental Procedures. smFISH to detect *nos* or *osk* mRNA was performed on mature, stage 14 oocytes dissected immediately after heat shock (t = 0 hr) or after being held for 18 hr due to nutrient deprivation (t = 18 hr). Scale bar, 25 μm.

(D) Quantification of smFISH experiments shown in (C) is presented. The total fluorescence intensity at the oocyte posterior (in arbitrary units) was determined for ≥20 oocytes per condition. Immediately after heat shock (0 hr), control and $Dmn^{OE}$ oocytes had a similar amount of *nos* or *osk* localized at the posterior cortex (blue circles). After 18 hr, the amount of localized *nos* or *osk* was significantly reduced in $Dmn^{OE}$ oocytes as compared to similarly aged control oocytes (pink circles; *nos*: $p = 5.2 \times 10^{-5}$; *osk*: $p = 7.2 \times 10^{-5}$). Furthermore, the amount of each RNA at the posterior was similar in 0 and 18 hr control oocytes, whereas $Dmn^{OE}$ oocytes showed significantly less localized *nos* or *osk* over time (compare 0 to 18 hr; *nos*: $p = 7.3 \times 10^{-6}$; *osk*: $p = 6.2 \times 10^{-6}$). Statistical analysis was performed using the Wilcoxon rank sum test. Red horizontal lines indicate median fluorescence.

(E) Wild-type females or females with *didum* mutant germline clones were subjected to the regimen shown in (B). smFISH to detect *nos* and *osk* mRNAs was performed on mature, stage 14 oocytes dissected from well-fed females (t = 0 hr) or after being held for 18 hr (t = 18 hr). Scale bar, 25 μm.

(F) Qualitative analysis of *nos* and *osk* mRNA localization is shown. Localization was categorized as strong if entirely cortical, intermediate if some cortical accumulation was observed, and weak/none for minimal cortical accumulation or an entirely diffuse pattern. A total of ≥37 oocytes were analyzed for *didum* mutants at each time point; ≥23 oocytes for wild-type at each time point. See Figure S2 for examples of each category.

See also Movie S6.

we show that such actin-dependent anchoring is not sufficient to maintain germ plasm at the posterior of the *Drosophila* oocyte. Rather, the localized state of *Drosophila* germ plasm is a dynamic one, with germ plasm RNP particles engaged in local dynein- and kinesin-mediated trafficking on cortical microtubules through the late stages of oogenesis. Moreover, this motility is important for the long-term retention of germ plasm at the cortex, thereby ensuring the integrity of the germ plasm

over extended periods of time and under conditions of environmental stress.

The antagonistic effect of MyoV on motility is consistent with a role in tethering RNP particles to cortical actin filaments. We envision that tethering is transient, such that persistent transport on short microtubules that course among the cortical actin meshwork is necessary to maintain a high local concentration of germ plasm components. Such plasticity could be important for reorganization of germ plasm RNP particles to promote translation of mRNAs like *nos* that initiates during oogenesis. Alternatively, it may facilitate the release of germ plasm RNP particles from the cortex that occurs after fertilization and is necessary for their inheritance by primordial germ cells.

## EXPERIMENTAL PROCEDURES

### Fly Stocks

The following mutants, mutant combinations, and transgenic lines were used: *y* $w^{67c23}$ (Lindsley and Zimm, 1992); *gfp-vas* (Johnstone and Lasko, 2004); *FRT42B* $Khc^{27}$ (Brendza et al., 2000); *FRT42B didum*$^{88}$ (Krauss et al., 2009); $Dhc^{6-10}/Dhc^{6-12}$ (Gepner et al., 1996); *hsp70>Dmn* (Duncan and Warrior, 2002); *UASp-MyoV-gfp* (Krauss et al., 2009); *UAS-EB1-GFP* (Rolls et al., 2007); *osk-(ms2)*$_6$ (Lin et al., 2008); *nos-(ms2)*$_{18}$ (Brechbiel and Gavis, 2008); and *hsp83-MCP-GFP* (Forrest and Gavis, 2003). *UAS* transgenes were expressed by crossing to *P(matα4-GAL-VP16)*$^{67}$; *P(matα4-GAL-VP16)*$^{15}$ (Hunter and Wieschaus, 2000). $Khc^{27}$ and *didum*$^{88}$ germline clones were generated by the *FLP/ovoD* method (Chou and Perrimon, 1996).

### Live Two-Photon 4D Imaging

Mated females were fed for 2 days at 25°C, ovaries were dissected in Schneider's medium, and individual egg chambers were isolated using tungsten needles. Egg chambers were transferred in Schneider's medium to a culture chamber created using a Secure-Seal spacer (Molecular Probes) on a glass slide, covered with a #1.5 coverslip, and imaged on a custom-built two-photon scanning microscope (Denk et al., 1990) built around an upright Olympus BX51 base. Images were taken with an excitation wavelength of 920 nm. Photons were collected both through a LUMPlanFI/IR 40×, 0.8 NA water-immersion objective (Olympus) and through a 1.3 NA oil-condenser lens, and detected with high quantum efficiency GaAsP photomultipliers (Hamamatsu). The MATLAB software ScanImage (Pologruto et al., 2003) was modified to control a piezo objective (PI). Stacks of five images, 128 × 64 pixels or 128 × 128 pixels corresponding to 512 or 973 $\mu m^2$ regions, taken at 1.5 μm steps were recorded every 1 or 1.5 s, respectively. Trail images were prepared in ImageJ by performing maximum projections on the time axis of image series (*xyt*) over a 100 s time window, unless otherwise noted. Kymographs were prepared in ImageJ by reslicing image series (*xyt*) along the y axis, and maximum projections were generated over a range of y values.

### Live Confocal Imaging and FRAP Analysis

Individual egg chambers were isolated as described above, mounted in glass-bottom dishes (MatTek), covered with a 1 $mm^2$ #1 coverslip, and cultured in Schneider's medium as described previously by Weil et al. (2006). Images were collected with a Leica SP5 confocal microscope using a 63×/1.4 NA oil-immersion objective. FRAP experiments were performed as previously described (Sinsimer et al., 2011). Images of EB1-GFP were captured at 1.4 frames/s for 30 s.

### Cytoskeleton Disruption

Stock solutions of inhibitors were prepared in 100% ETOH. Egg chambers were cultured in Schneider's media containing 0.5 μM latA (Sigma-Aldrich) or 50 μg/ml colcemid (Sigma-Aldrich) (Forrest and Gavis, 2003; Weil et al., 2006). An equivalent volume of 100% ETOH was added to the medium for mock-treated controls. Similar results (not shown) were obtained using cytochalasin D to disrupt actin and colchicine to disrupt microtubules.

### Manual Quantification of Particle Dynamics

To calculate net displacement of germ plasm particles, 100 s image series (*xyt*) from three independent oocytes were quantified for each genotype. Pixel coordinates for each particle's first and last appearance in the image series were manually identified in ImageJ (1.44o; NIH) and used to calculate net displacement in Microsoft Excel. Plots were prepared using Prism (GraphPad), and statistical analyses were performed using MATLAB (R2011a; MathWorks). The average velocity of a particle was approximated by measuring particle displacement during short periods of sustained, linear movement and dividing by the time period.

### Semiautomated Quantification of Particle Dynamics

For all analyses, 100 s image series (*xyt*) from each of three oocytes were quantified. An initial filtering step was performed using the ImageJ plugin "A trous" wavelet filter, and particles were identified using spot-detection software available for MATLAB (spotDetector; Danuser Lab). Coefficients for the initial wavelet filter and spotDetector were empirically chosen to optimize particle detection. Tracks were then identified using the MATLAB package u-track (Jaqaman et al., 2008). Minor adjustment from default coefficients improved track assignment, but manual curation was still required to completely remove aberrant tracks. Displacement and instantaneous velocity measurements were extracted, and a 1D median filter (over time) was applied to eliminate the influence of spurious measurements when determining maximum values. An "immotile" fraction was defined based on analysis of colcemid-treated GFP-Vas samples, in which directed movements were rare. Outliers in maximum displacement and maximum instantaneous velocity measurements were identified based on interquartile ranges of all identified particles; the threshold for the immotile population was subsequently chosen to exclude these outliers.

### Dmn Overexpression Experiments

#### *Motility Analysis*

Wild-type females and females carrying the *hs>Dmn* transgene were mated to wild-type males and fed for 2 days at 25°C, then transferred to empty vials and heat shocked for 1 hr at 37°C. After a 30 min recovery period at room temperature, a second 30 min heat shock was administered. Heat shock flies were transferred to yeasted vials and aged for 6 hr to allow expression of Dmn protein. Ovaries were then dissected, and individual egg chambers were cultured for live two-photon imaging as described above.

#### *Analysis of Germ Plasm Retention in Mature Eggs*

Wild-type females and *hs>Dmn* transgenic females were heat shocked as described above. For each genotype, ovaries were dissected from half of the females immediately following heat shock (t = 0 hr) and fixed for smFISH as described below. The remaining females were induced to hold eggs by transferring them without males to vials containing only a moistened Kimwipe. Ovaries were dissected after 18 hr of food deprivation (t = 18 hr) and fixed for smFISH. For quantification of mRNA localization, the total fluorescence intensity of *nos* and *osk* RNA at the posterior of each oocyte in the plane with maximum intensity was determined using ImageJ and MATLAB and plotted using Prism 5.0 (n > 20 for each genotype).

### smFISH

Ovaries were dissected into PBS and fixed in 4% electron microscopy grade formaldehyde (Polysciences) for 30 min. Samples were then washed 3 × 5 min in PBST (PBS/0.1% Tween 20) and stepped into methanol. FISH was performed as described previously by Little et al. (2011) and Raj et al. (2008) using probes for the coding region of *nos* or *osk* conjugated to ATTO dyes (ATTO-Tec). Oocytes shown in Figure 4C were imaged using a Leica SPE confocal microscope with a 40×/1.25 NA oil-immersion objective; oocytes shown in Figure 4E were imaged on a Leica SP5 confocal microscope using a 63×/1.3 NA glycerol objective.

## SUPPLEMENTAL INFORMATION

Supplemental Information includes two figures, one table, and six movies and can be found with this article online at http://dx.doi.org/10.1016/j.celrep.2013.10.045.

## ACKNOWLEDGMENTS

We thank S. Little for kindly providing the *osk* probe, advice on probe preparation and smFISH, and suggesting the nutrient deprivation experiment. We are grateful to T. Chou, A. Ephrussi, P. Lasko, W. Saxton, R. Warrior, M. Welte, E. Wieschaus, and the Bloomington Stock Center for fly stocks. We thank E. Abbaszadeh and B. Bhogal for comments on the manuscript. This work was supported by grants from the National Institutes of Health to K.S.S. (F32GM087005) and E.R.G. (R01GM067758) and the Lewis-Sigler Institute for Integrative Genomics (P50GM071508).

Received: June 25, 2013
Revised: September 11, 2013
Accepted: October 28, 2013
Published: November 27, 2013

## REFERENCES

Babu, K., Cai, Y., Bahri, S., Yang, X., and Chia, W. (2004). Roles of Bifocal, Homer, and F-actin in anchoring Oskar to the posterior cortex of *Drosophila* oocytes. Genes Dev. *18*, 138–143.

Becalska, A.N., and Gavis, E.R. (2009). Lighting up mRNA localization in *Drosophila* oogenesis. Development *136*, 2493–2503.

Brechbiel, J.L., and Gavis, E.R. (2008). Spatial regulation of *nanos* is required for its function in dendrite morphogenesis. Curr. Biol. *18*, 745–750.

Brendza, R.P., Serbus, L.R., Duffy, J.B., and Saxton, W.M. (2000). A function for kinesin I in the posterior transport of *oskar* mRNA and Staufen protein. Science *289*, 2120–2122.

Cha, B.J., Serbus, L.R., Koppetsch, B.S., and Theurkauf, W.E. (2002). Kinesin I-dependent cortical exclusion restricts pole plasm to the oocyte posterior. Nat. Cell Biol. *4*, 592–598.

Chou, T.B., and Perrimon, N. (1996). The autosomal FLP-DFS technique for generating germline mosaics in *Drosophila melanogaster*. Genetics *144*, 1673–1679.

Delanoue, R., and Davis, I. (2005). Dynein anchors its mRNA cargo after apical transport in the *Drosophila* blastoderm embryo. Cell *122*, 97–106.

Delanoue, R., Herpers, B., Soetaert, J., Davis, I., and Rabouille, C. (2007). *Drosophila* Squid/hnRNP helps Dynein switch from a *gurken* mRNA transport motor to an ultrastructural static anchor in sponge bodies. Dev. Cell *13*, 523–538.

Denk, W., Strickler, J.H., and Webb, W.W. (1990). Two-photon laser scanning fluorescence microscopy. Science *248*, 73–76.

Duncan, J.E., and Warrior, R. (2002). The cytoplasmic dynein and kinesin motors have interdependent roles in patterning the *Drosophila* oocyte. Curr. Biol. *12*, 1982–1991.

Forrest, K.M., and Gavis, E.R. (2003). Live imaging of endogenous RNA reveals a diffusion and entrapment mechanism for *nanos* mRNA localization in *Drosophila*. Curr. Biol. *13*, 1159–1168.

Fusco, D., Accornero, N., Lavoie, B., Shenoy, S.M., Blanchard, J.M., Singer, R.H., and Bertrand, E. (2003). Single mRNA molecules demonstrate probabilistic movement in living mammalian cells. Curr. Biol. *13*, 161–167.

Gepner, J., Li, M., Ludmann, S., Kortas, C., Boylan, K., Iyadurai, S.J., McGrail, M., and Hays, T.S. (1996). Cytoplasmic dynein function is essential in *Drosophila melanogaster*. Genetics *142*, 865–878.

Hammer, J.A., 3rd, and Sellers, J.R. (2012). Walking to work: roles for class V myosins as cargo transporters. Nat. Rev. Mol. Cell Biol. *13*, 13–26.

Hunter, C., and Wieschaus, E. (2000). Regulated expression of *nullo* is required for the formation of distinct apical and basal adherens junctions in the *Drosophila* blastoderm. J. Cell Biol. *150*, 391–401.

Jankovics, F., Sinka, R., Lukácsovich, T., and Erdélyi, M. (2002). MOESIN crosslinks actin and cell membrane in *Drosophila* oocytes and is required for OSKAR anchoring. Curr. Biol. *12*, 2060–2065.

Jaqaman, K., Loerke, D., Mettlen, M., Kuwata, H., Grinstein, S., Schmid, S.L., and Danuser, G. (2008). Robust single-particle tracking in live-cell time-lapse sequences. Nat. Methods *5*, 695–702.

Johnstone, O., and Lasko, P. (2004). Interaction with eIF5B is essential for Vasa function during development. Development *131*, 4167–4178.

King, M.L., Messitt, T.J., and Mowry, K.L. (2005). Putting RNAs in the right place at the right time: RNA localization in the frog oocyte. Biol. Cell *97*, 19–33.

Krauss, J., López de Quinto, S., Nüsslein-Volhard, C., and Ephrussi, A. (2009). Myosin-V regulates *oskar* mRNA localization in the *Drosophila* oocyte. Curr. Biol. *19*, 1058–1063.

Lantz, V.A., Clemens, S.E., and Miller, K.G. (1999). The actin cytoskeleton is required for maintenance of posterior pole plasm components in the *Drosophila* embryo. Mech. Dev. *85*, 111–122.

Lerit, D.A., and Gavis, E.R. (2011). Transport of germ plasm on astral microtubules directs germ cell development in *Drosophila*. Curr. Biol. *21*, 439–448.

Lin, M.D., Jiao, X., Grima, D., Newbury, S.F., Kiledjian, M., and Chou, T.B. (2008). *Drosophila* processing bodies in oogenesis. Dev. Biol. *322*, 276–288.

Lindsley, D.L., and Zimm, G.G. (1992). The Genome of *Drosophila melanogaster* (San Diego: Academic Press).

Little, S.C., Tkačik, G., Kneeland, T.B., Wieschaus, E.F., and Gregor, T. (2011). The formation of the Bicoid morphogen gradient requires protein movement from anteriorly localized mRNA. PLoS Biol. *9*, e1000596.

López de Heredia, M., and Jansen, R.P. (2004). mRNA localization and the cytoskeleton. Curr. Opin. Cell Biol. *16*, 80–85.

Mahowald, A.P. (2001). Assembly of the *Drosophila* germ plasm. Int. Rev. Cytol. *203*, 187–213.

Martin, K.C., and Ephrussi, A. (2009). mRNA localization: gene expression in the spatial dimension. Cell *136*, 719–730.

McGrail, M., and Hays, T.S. (1997). The microtubule motor cytoplasmic dynein is required for spindle orientation during germline cell divisions and oocyte differentiation in *Drosophila*. Development *124*, 2409–2419.

Medioni, C., Mowry, K., and Besse, F. (2012). Principles and roles of mRNA localization in animal development. Development *139*, 3263–3276.

Polesello, C., Delon, I., Valenti, P., Ferrer, P., and Payre, F. (2002). Dmoesin controls actin-based cell shape and polarity during *Drosophila melanogaster* oogenesis. Nat. Cell Biol. *4*, 782–789.

Pologruto, T.A., Sabatini, B.L., and Svoboda, K. (2003). ScanImage: flexible software for operating laser scanning microscopes. Biomed. Eng. Online *2*, 13.

Raj, A., van den Bogaard, P., Rifkin, S.A., van Oudenaarden, A., and Tyagi, S. (2008). Imaging individual mRNA molecules using multiple singly labeled probes. Nat. Methods *5*, 877–879.

Rolls, M.M., Satoh, D., Clyne, P.J., Henner, A.L., Uemura, T., and Doe, C.Q. (2007). Polarity and intracellular compartmentalization of *Drosophila* neurons. Neural Dev. *2*, 7.

Sinsimer, K.S., Jain, R.A., Chatterjee, S., and Gavis, E.R. (2011). A late phase of germ plasm accumulation during *Drosophila* oogenesis requires lost and rumpelstiltskin. Development *138*, 3431–3440.

Theurkauf, W.E., Smiley, S., Wong, M.L., and Alberts, B.M. (1992). Reorganization of the cytoskeleton during *Drosophila* oogenesis: implications for axis specification and intercellular transport. Development *115*, 923–936.

Vanzo, N., Oprins, A., Xanthakis, D., Ephrussi, A., and Rabouille, C. (2007). Stimulation of endocytosis and actin dynamics by Oskar polarizes the *Drosophila* oocyte. Dev. Cell *12*, 543–555.

Weil, T.T., Forrest, K.M., and Gavis, E.R. (2006). Localization of *bicoid* mRNA in late oocytes is maintained by continual active transport. Dev. Cell *11*, 251–262.

Woolner, S., and Bement, W.M. (2009). Unconventional myosins acting unconventionally. Trends Cell Biol. *19*, 245–252.

Wyman, R. (1979). The temporal stability of the *Drosophila* oocyte. J. Embryol. Exp. Morphol. *50*, 137–144.